

# **Chapter 3**

---

---

## **Materials and Methods**

---

---



This chapter describes the application of the Design of Experiments using Taguchi's approach for parameter selection, experimental design and to conduct experiments for optimization of mechanical properties. The experimental details involved, GMAW welding based on Taguchi's  $L_{16}$  orthogonal array has been detailed thoroughly.

The chapter concludes with the details of  $L_{16}$  orthogonal array used and characterization techniques involved for the present investigation.

### **3. Materials and Method**

#### **3.1 Introduction**

In this chapter, GMAW welding, preliminary trials and experimentation conducted on A572 gr. 50 and 316L stainless steels for variable welding current, weld speed and shielding gas flow rates is discussed in detail. Preliminary trials were utilized to identify the limits of experimentation for full penetration in a single pass with pre-mixed shielding gas of Ar+CO<sub>2</sub> to get the full depth of penetration in a single pass. In the Design of Experiment, Taguchi's approach was used to select levels and optimize the results, followed by validation through macrostructure, microstructure, hardness and tensile tests. Effects of various conditions along with their contribution on Heat Affected Zone was used to analyse and improve the HAZ microstructure and mechanical properties.

#### **3.2 Research Methodology**

In order to study the behaviour of heat affected zone under different welding conditions on A572 gr. 50 and 316L stainless steel specimens were fabricated under different currents, shielding gas flow rate and welding speed by Gas Metal Arc Welding. HAZ is heavily affected by uniformity in experimentation and finding the key features that push the weld's quality to the optimum levels for single-pass welding is critical. HAZ structure significantly affects the quality of weld and service life of the welded structure. Pre-heat and post-heat treatments are among the ways to enhance the HAZ and Weld life, but it puts a heavy constrain on heat treatments for bigger structural joints. The experimentation was carried out in three stages. The methodology of research for the accomplishment of investigation and research objectives three-phased structure has been used. The flow chart for the scheme of research is shown in Figure 3.1.

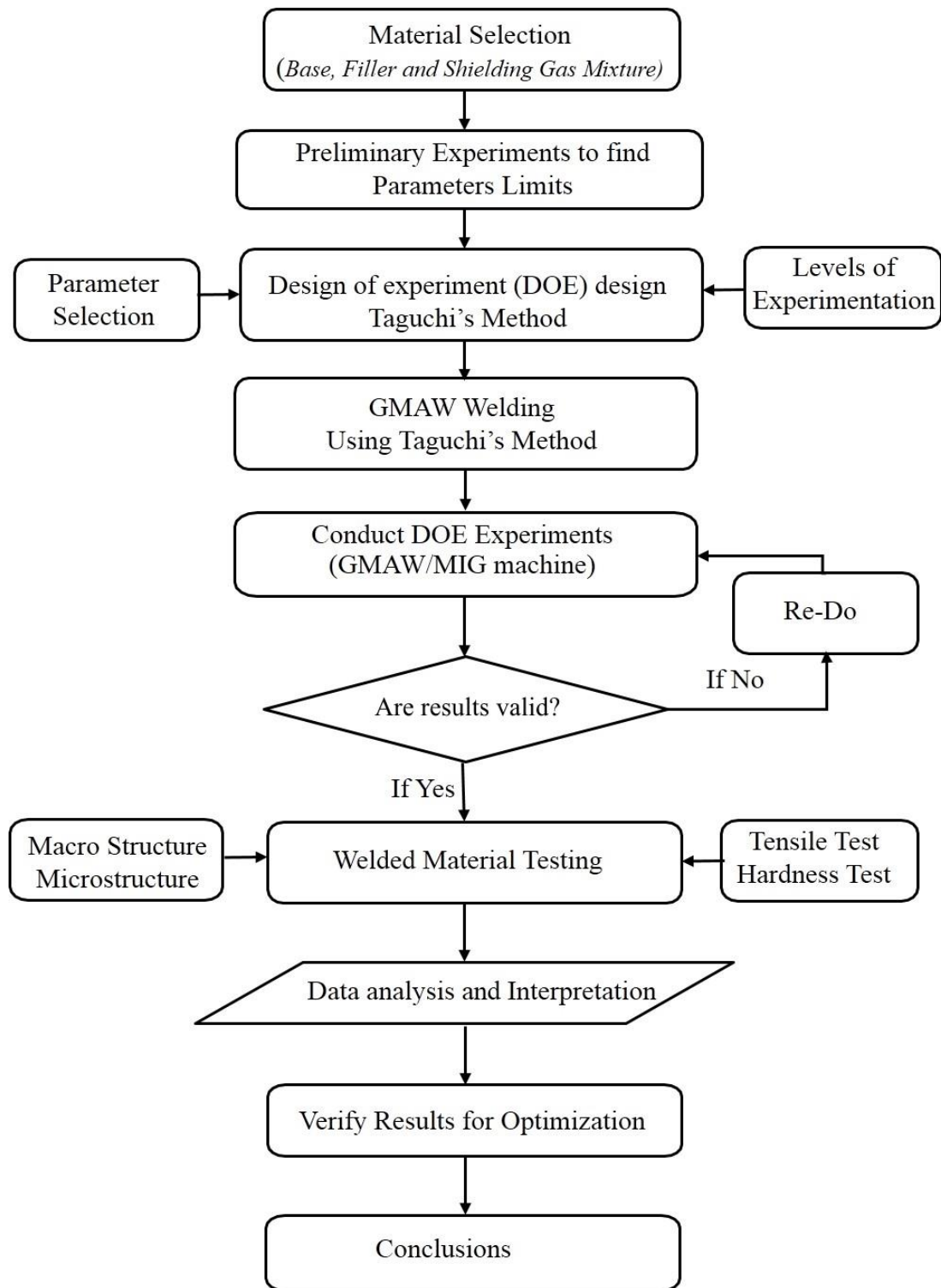


Figure 3.1: Flow-chart for the scheme of work

The first phase consists of material selection and finds the limits of welding parameters for fabrication to identify various levels of Current, Weld speed and Shielding gas flow rate for pre-mixed Ar+CO<sub>2</sub> for the single-pass weld. A strategy would be adopted to identify the different levels of selected parameters through trial experiments and define

the limits of experimentation, considering full penetration along with defect-free and minimum spatter quantity. As optimum reinforcement considering bead width to penetration ratio of 2:1 has been found to be best for welding [134].

The second stage of the research plan will comprise the application of Design of Experiments using Taguchi's approach with the help of MINITAB 17 software to select orthogonal array and perform the experiments from preliminary experiments results. Design of experiments (DOE) techniques would be utilized to develop the experimental plan, and ANOVA (analysis of variance) would be used to isolate the effect of each tested parameter upon response variables (i.e., components of weld geometry, HAZ and weld strength). Numerical optimization would be carried out to find the most influential parameter needed to be controlled and optimize the influential parameters to minimise or maximise the response variables. It would be followed by experimentation and optimization of welding process parameters and their effect on HAZ. The ANOVA results will be used to develop the mathematical model to analyze weld joint quality and improve mechanical strength.

The third stage of research work will focus on validating the optimum results with results obtained from DOE experimentation. HAZ contribution for maximum joint strength and microstructural changes in and around the HAZ will be correlated and analyzed.

### **3.3 Material Selection for Base Materials, Filler Wire and Shielding Gas**

A572 gr. 50 (HSLA) steel is the best replacement for commercially viable mild steel with the added value of high strength. Its use can enable substantial savings in structural weight and material costs. Another grade of material that has immunity from most environmental oxidations/corrosion is Stainless steel being used in severely corrosive environments. The various material for experimentation in the form of the plate

(BM) and spool (filler/electrode) from various companies has been procured and tabulated in table no 3.1.

Table 3.1: Procured Materials

Items	Procurement details
A572 grade 50 plate	Steel Mart, Byculla West, Mumbai in plate form of thickness 5 mm and 50 mm width
316L Stainless Steel plate	Steel Mart, Byculla west, Mumbai in plate form of thickness 5 mm and 50 mm width
ER 316L Spool	D&H Secheron company, Autotherm 316L, MIG welding wire with dia. 1.2 mm
AWS A5.18:ER70S-6 Spool	Manohar MIG welding wire with dia 1.2 mm

### 3.3.1 Base Materials A572 grade 50

High strength low alloy steel is replacing the widely used mild steel due to its strength and corrosion-resistant properties. Specific mechanical properties/chemical properties can be achieved by microalloying. ASTM A572 is a High Strength Low Alloy Columbium-Vanadium Structural Steel grade for plates. A572 has a family of five grades with specified minimum yield strengths of 289, 344, 379, 413 and 448 MPa, respectively. A572 gr. 50 grade is having wide applications in offshore structures, shipbuilding, bridges, oil/gas vessels, agricultural and construction machines etc. [135, 136]. The chemical composition of base metal and filler material has been tabulated in Table 3.2. The GMAW process can accommodate a base plate thickness of 0.5 to 15 mm [137].

Table 3.2: Chemical composition (Wt. %) of A572 gr. 50 and filler material

Elements	C	Si	Mn	Mo	Cr	P	S	Ni	V	Cd	Co	Fe
A572 gr. 50	0.08	0.4	0.95	0.02	0.02	0.02	0.01	0.015	0.001	0.001	0.002	Balance
Filler, ER70S-6	0.12	1.25	0.85	-	-	0.05	0.03	-	-	-	-	Balance

For the fabrication of large and complex structures, the weld joint strength is also affected by the direction of rolling and grain size [138]. However, the weld strength is affected by the rolling direction of base metal and other metallurgical properties.

**3.3.2 Base Materials 316L Stainless Steel**

316L stainless steel possesses the second-largest share of applications from domestic to industrial applications, and its demand is increasing year by year. Stainless steel 316L (low carbon) is best for the highly corrosive environment and is resistant to sensitization problems. In 316L steel, lesser carbon (less than 0.02%) is available to react with chromium and create chromium depleted zones which are prone to corrosion. It contains Mo and has a greater resistance to chemical attack with respect to other Stainless Steel (SS) steel grades. It's considerably more resistant to solutions of sulfuric acid, chlorides, bromides, iodides and fatty acids at high temperatures. Improper welding parameters and weld conditions increase the loss of chromium, resulting in localized corrosion and failure of joints. A higher percentage of C in filler may also create the chromium depleted zone, causing sensitization. Typical failures, like distortion, HAZ cracks and corrosion, have been found in areas having segregation of alloys.

**3.3.3 Filler Material**

The filler metals were chosen based on their compatibility with the parent metals. In this study, different filler metals for A572 grade and 316L SS have been chosen and are either matching or slightly over alloyed. For A572 gr. 50 filler wire of mild steel copper coated electrode has been used for experimentation which is slightly over alloyed. As it is known to provide minimum spatter and stable arc during MIG/GMAW under optimum welding conditions [52]. It is an acceptable interpretation that slightly over alloyed filler metal with equal or slightly higher tensile strength with respect to base metal should be used [53]. A filler in the form of a spool was procured, and its chemical composition has been determined using spark spectroscopy and has been tabulated in Table 3.2. Improper welding parameters causing excessive loss of chromium and a higher percentage of carbon in filler may also create Cr depletion, promoting sensitization. So

low carbon version of 316 SS has been selected to avoid sensitization problems. Low carbon eliminates/retards the chromium carbide formation and avoids sensitization.

Table 3.3: Chemical composition (Wt. %) of 316L SS and ER 316L filler material

Elements	C	Si	Mn	Mo	Cr	P	S	Ni	Cu	Nb	Co	Ti	Fe
<b>316L SS</b>	0.0284	1.00	1.30	2.11	17.2	0.003	0.005	11.4	0.342	0.0473	0.158	0.0063	Balance
<b>Filler, ER 316L</b>	0.03	1.20	1.25	2.0	16.5	0.003	0.005	10.5	-	-	-	-	Balance

Similarly, for the 316L SS base material matching electrode, ER 316L has been selected for welding. The chemical composition of base metal and filler material has been tabulated in Table 3.3 as it forms joints with similar properties across the weld joint.

### 3.3.4 Shielding Gas

CO<sub>2</sub> has been widely used as shielding Gas for HSLA, and mild steels with a larger amount of spatter and poor surface quality and use of a mixture of Ar and CO<sub>2</sub> not only reduced spatter but improved the surface appearance by minimising the requirement of post-cleaning. One of the key factors that affect the mode of transfer, the microstructure and mechanical properties of the welds is the shielding gas. A mixture of CO<sub>2</sub> and Ar is also used as the shielding gas for the GMAW process for various steels [139-141]. The CO<sub>2</sub> percentage in shielding gas has increased weld penetration levels. For austenite stainless steel in GTA welding with a mixed supply of shielding gas it was found to increase the welding quality along with reduction in the energy level by 20% and the emission rate of hazardous fumes [142, 143]. CO<sub>2</sub> has the ability to constrict arc plasma and hence increases current density near the arc axis. It was concluded that CO<sub>2</sub> GMA would have excellent energy source properties comparable to that of He and Ar [52, 53].

## 3.4 Fabrication of A572 grade 50 and 316L Stainless Steel

The GMAW process with a consumable electrode and Direct Current Electrode positive polarity is used for HSLA and Stainless Steels. But special care should be taken for stainless steel to avoid defects in and around the weld bead. So automatic GMAW

machine of ESAB RC-AUTO-K400 was used along with a variable speed MAXIMIG 251 trolley (10mm/sec Max.) with fixture as shown in Figure 3.2 for experimentation. Speed measurement of filler wire was also carried out. The filler wire was allowed to run without striking the arc, i.e. away from the workpiece. The length of the wire was calculated after running it for 15 seconds by stopwatch and then converted in terms of mm/sec. Similarly, trolley speed was also calculated during and after weld completion. The actual setup used for experimentation is shown in Figure 3.2.

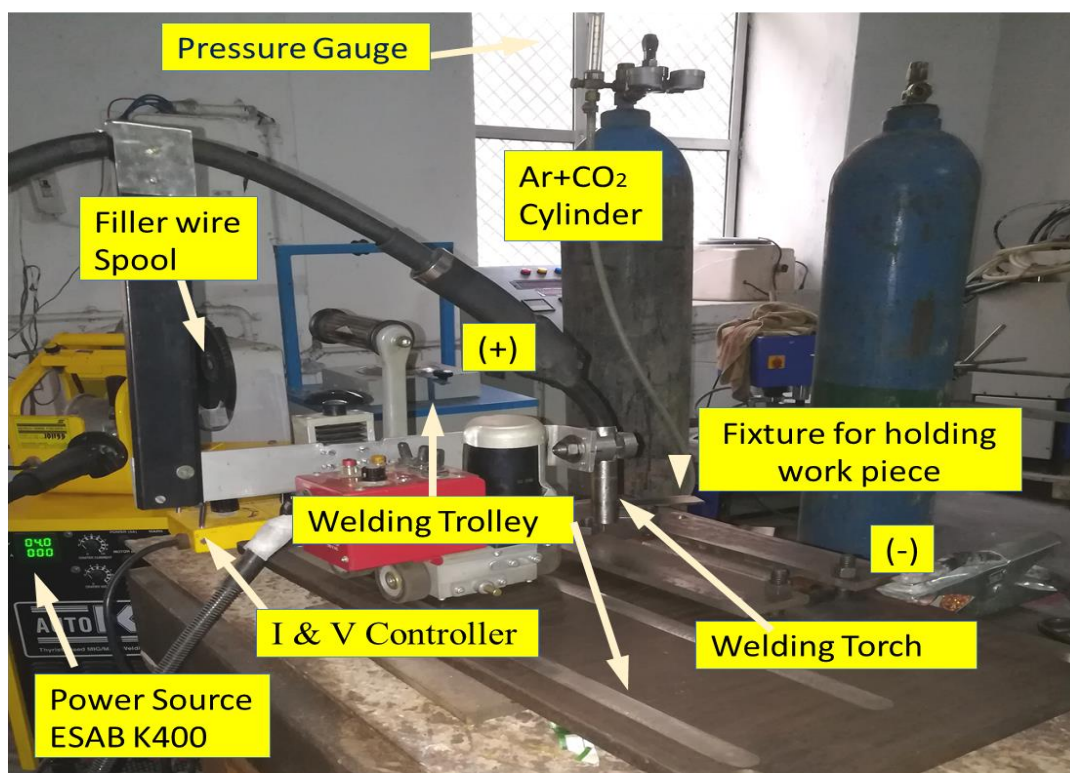


Figure 3.2: Experiment setup used for GMAW

GMAW machine contained independent regulators for current and voltage controls. In the present work, 316L SS and A572 gr. 50 flats of thickness 5 mm was used. The schematic diagram of steps followed during the fabrication process is shown in Figure 3.3(a-f).

In this analysis, the specimens were machined to a single V-edge of 30° on a milling machine using a milling cutter. The included angle was 60° with a root gap of 1.2

mm (approx.) and land of 1.2 mm (approx), as shown in Figure 3.3 c. Special spacers have been used to maintain the root gap before and after welding.

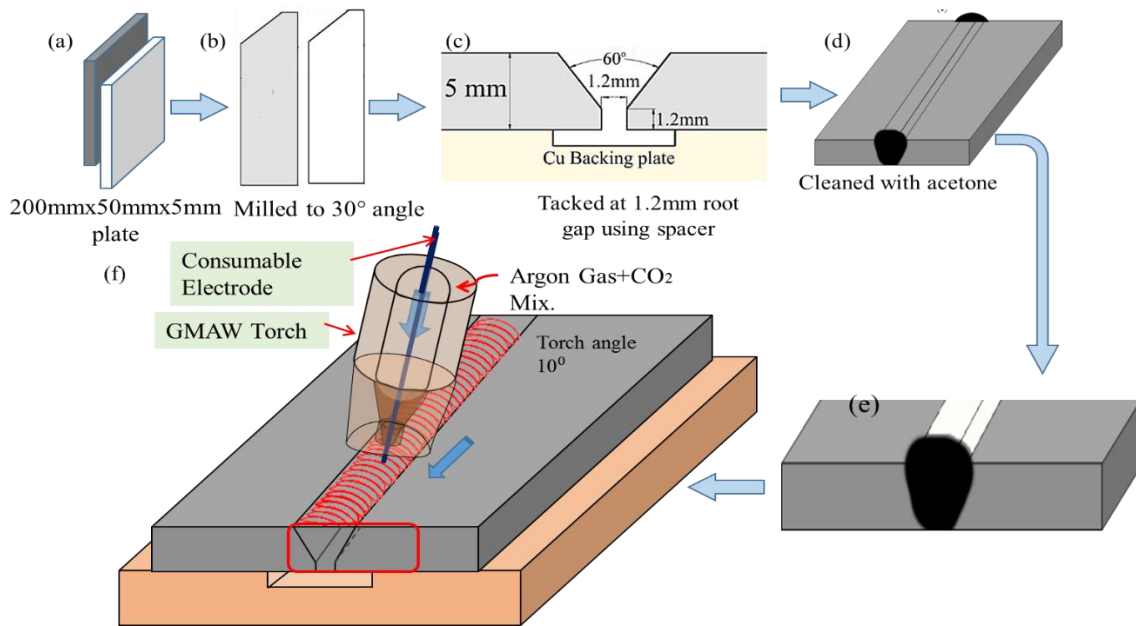


Figure 3.3: Schematic view of steps followed during fabrication process  
 a) Size reduction, b) Milling 30° angle, c) Fixing of root gap, d) Tacking,  
 e) Cleaning and f) GMAW welding at various levels

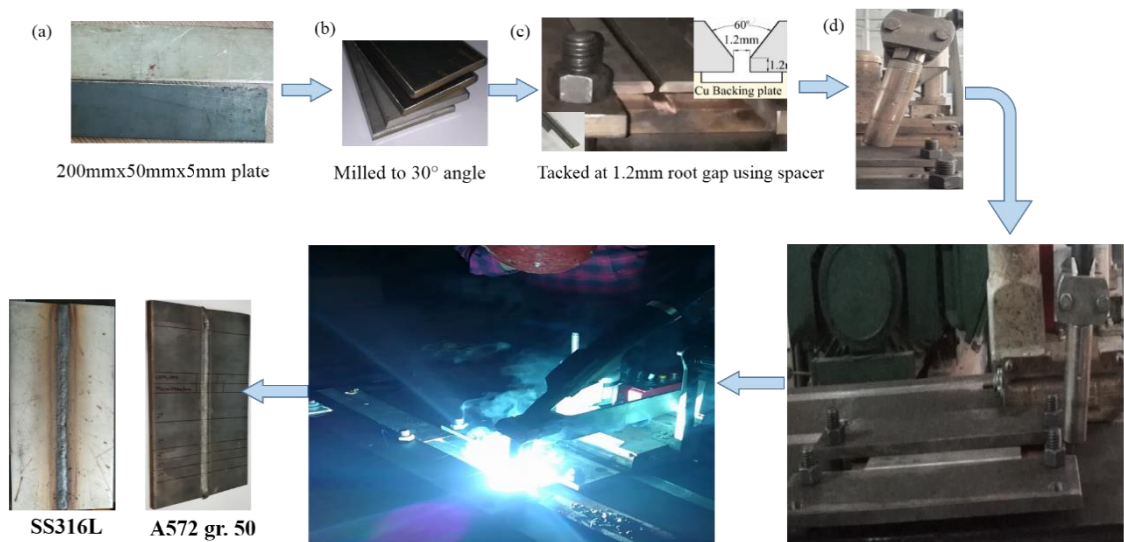


Figure 3.4: Steps followed during fabrication a) Cleaned base b) Milled specimen, c) joint configuration, d) fixed 10° torch angle, e) Start of Welding, f) GMAW

After tack welding at both ends, further grinding was carried out to get the V-groove butt joint configuration and remove the unwanted material and burrs. Actual pics of steps followed, tools used and welded specimens have been shown in Figure 3.4(a-f).

### 3.4.1 Finding the limits of the experiment through trial runs.

Preliminary experiments were carried out to find the Limits of experimentations and levels for Taguchi’s analysis for Current, Weld speed and Gas flow rate in single pass welding with a pre-mixed shielding gas mixture of Ar and CO<sub>2</sub>. Low current values showed a lack of penetration in few samples with higher weld speed while higher showed excessive reinforcement for both materials. Heavy oxidation was found for a low gas flow rate, as shown in Figure 3.5(a-d). The trial runs have been used to decide the levels for experimentation.

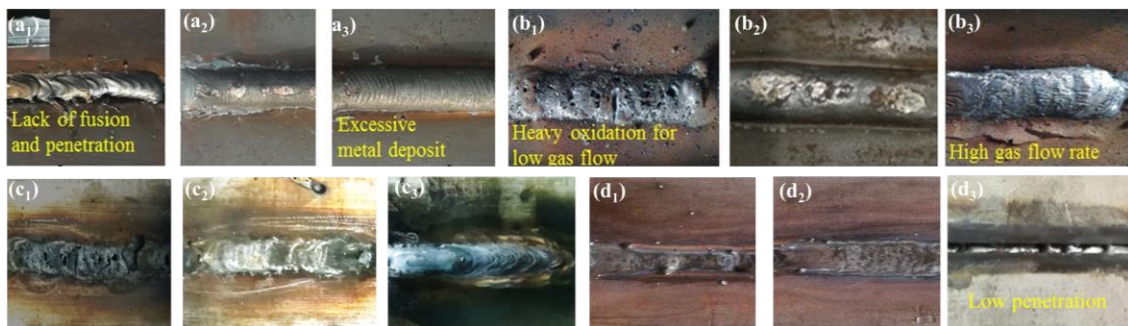


Figure 3.5: Setting the limits of welding parameters a) Current for A572, b) Gas flow rate for A572, c) Current for 316L, d) Gas flow rate for 316L

### 3.4.2 Finding the Levels of Experimentation

DOE using Taguchi’s approach has become a much more attractive tool to practising engineers and scientists, and since the last four decades, there have been limitations when conventional experimental design techniques were applied to industrial experimentation. Taguchi approach, also known as orthogonal array design, adds a new dimension to conventional experimental design with the added advantage of lesser experimentation cost and time-saving. Taguchi method is a broadly accepted method of DOE, which has proven to create high-quality products at a relatively lower low cost of experimentation and time-saving. It’s a statistical technique used to study and analyze the effect of various process parameters on the response. Taguchi’s analysis was used to optimize and find the optimum levels of current gas, flow rate and weld speed. MINITAB 17 software using Taguchi’s approach was used, and four levels for Current, Gas flow

rate and Weld Speed were selected for welding of A572 gr. 50 and 316L SS and Taguchi's L<sub>16</sub> orthogonal array has been chosen.

For welding A572 gr. 50 steel, various levels of current, gas flow rate and weld speed have been selected and tabulated in Table 3.4 with pre-mixed shielding gas of 82% Ar and 18% CO<sub>2</sub>. Other constant parameters were the torch angle of 10°, Work to contact tube distance of 15 mm, and filler diameter of 1.2 mm with copper as a backing plate.

Table 3.4: A572 gr. 50 Parameters According Taguchi's L<sub>16</sub>

Parameters	Level 1	Level 2	Level 3	Level 4
Current (Amp)	100	135	170	205
Gas flow rate (l/min)	10	14	18	20
Welding Speed (mm/sec)	1.25	2.50	3.75	5.00

Similarly, for welding 316L SS various selected parameters are tabulated in Table 3.5 with pre-mixed shielding gas of 88% Ar and 12% CO<sub>2</sub>. Other constant parameters were the same as for A572 gr.50, as stated earlier.

Table 3.5: SS 316L Parameters According Taguchi's L<sub>16</sub>

Parameters	Level 1	Level 2	Level 3	Level 4
Current (Amp)	95	120	145	170
Gas flow rate (l/min)	10	13	16	19
Welding Speed (mm/sec)	1.5	2.0	2.5	3.00

In addition to this, the results have been verified using microstructure, macrostructure, tensile and hardness tests to find the major constituents which affect the quality of the product. Weld bead quality plays an important role in determining the mechanical properties of a weld. The welding process parameters were the input variables, while the YS and UTS and Heat input were the output variables of the GMAW welding process. A single-pass welding process was used. By studying the effect of individual factors on the results, the best factor combination was determined, and the contribution of HAZ was studied using optical microscopy and mechanical properties.

The Design of Experiment and optimization technique followed by microstructural and mechanical properties analysis can give the best results in a cost-effective way.

### 3.5 Characterization

Samples were extracted from GMAW welded plates for various characterizations from the locations, as shown in Figure 3.6.

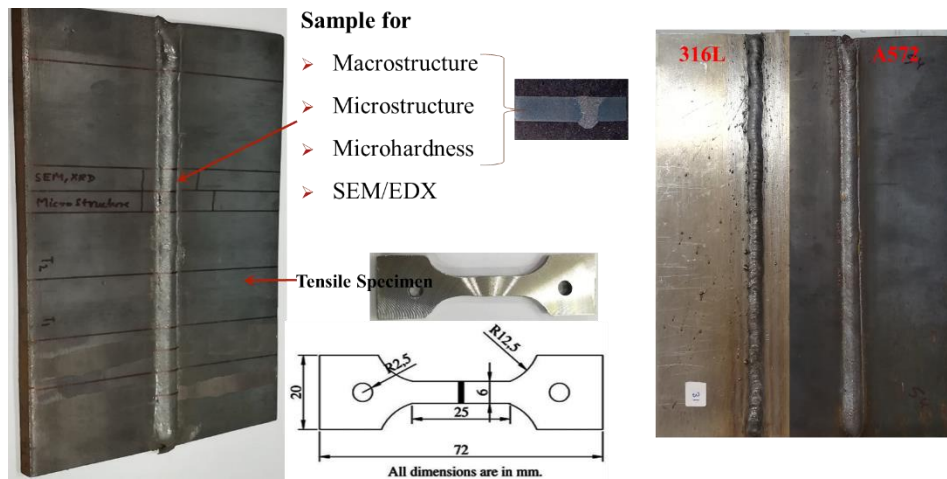


Figure 3.6: Location of extracted samples for various characterizations

#### 3.5.1 Optical Metallography

Specimens were prepared according to standard metallographic procedure (ASTM E3-11), i.e. grinding (SiC emery papers from 160, 200, 400, 600, 800, 1200, 1500, 2000 and 2500 micron starting with the roughest till finest grade) at the speed range of 200 to 300 rpm followed by mechanical polishing (with diamond paste for 316L only). The chemical etching with Nital (98% Ethonal+2% HNO<sub>3</sub>) was carried out for A572 gr. 50 for 20-30 seconds to reveal the grain boundaries. While for 316L stainless steel, Aqua Regia reagent (mixture of HNO<sub>3</sub> and HCl in the molar ratio of 1:3 respectively) was used for etching for 5-10 seconds. The chemically etched samples were observed under optical microscopy (Leitz Metallux-3), and the grain size distribution was analyzed through ImageJ software.

### 3.5.2 Microhardness

Vickers microhardness test was used to find out the change in hardness across the weld joint. Vickers Microhardness tester Model- MINIFLEX 600 DETEX ULTRA, Japan was used for microhardness test. Polished samples were carefully used so that the indentation due to diamond-shaped indent can be clearly visualized in the microscope enclosed with the machine. A load of 300 grams for 10 seconds of dwell time was used for both materials. Indentations were taken at 2 mm below the top surface along a transverse section at an interval of 0.5 mm in both materials as shown in Figure 3.7.

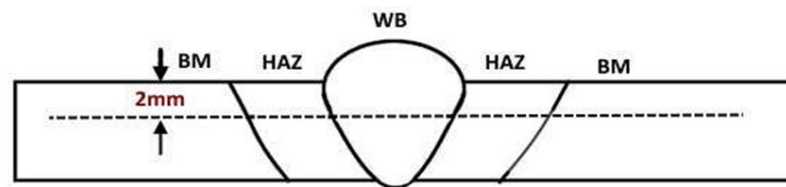


Figure 3.7: Location of hardness measurement across welded joints

### 3.5.3 Tensile Test

Tensile test specimen fabricated as per ASTM E8 from the welded workpiece as shown in Figure 3.6 [144]. Dog-bone-shaped tensile specimens of 25 mm gauge length, 6 mm gauge width and 4 mm gauge thickness were first cut by power hacksaw and then machined on a CNC machine (EMCO make). The test pieces were so long to ensure that the neck formation should not take place near the ends. Any surface regularities were removed using emery paper up to 800 grit size before testing the pieces. Tensile tests were carried out with a strain rate of 0.0006 per second (crosshead speed of 1 mm/min) on a computerized screw-driven Instron™ Universal Testing Machine (Model 4206) at room temperature. The tensile properties data for each condition was obtained, averaging three test results. Figure 3.8 shows the actual tensile test specimen fabricated under different welding conditions of base material and different levels of current for 316L SS and A572 gr. 50 before fracture.



Figure 3.8: Base and Welded Tensile test specimens of 316L SS and A572 gr. 50

### 3.5.4 Scanning Electron Microscopy (SEM)

For SEM analysis, the samples were also extracted precisely in a similar manner as it was taken out for optical microscopy. The dimensions of the specimens were 5 mm x 30 mm x 6 mm. Specimens were first polished on different grades of emery papers (400~2500 grit size), and then it was mechanically polished. The samples were not chemically etched as it was done in the case of optical microscopy. The mechanically polished samples were observed on SEM (Serial no. EVO18-20-45, ZEISS EVO 18 research, Germany). The fracture behaviour of the samples resulting from tensile testing was characterized using SEM.

The results obtained from different tests are presented in the next chapters.